SUPPLEMENTAL METHODS

LC-MS/MS analysis

Samples were analyzed by LC-MS/MS using a Dionex Ultimate 3000 rapid separation LC nanoUPLC system (Thermo Scientific) coupled with either an Orbitrap Fusion Tribrid, Orbitrap Lumos, or Orbitrap Q Exactive mass spectrometer (Thermo Scientific), as described below. For the five unlabeled samples analyzed by the Orbitrap Fusion Tribrid mass spectrometer (Figure S5), peptides were loaded onto a PepMap C18 nano trapping column (5 µm particle, 100 µm × 20 mm, Thermo Scientific) at 20 µL/min with 0.5% formic acid and then separated on a PepMap C18 analytical column (2 µm, 75 µm × 250 mm, Thermo Scientific) with a gradient of 2% to 35% acetonitrile in 0.1% formic acid over 60 minutes at a flow rate of 300 nL/min. All *m/z* values of eluting ions (range between 375-1575 Da) were measured at a resolution of 120,000. The MS1 scan was followed by data-dependent MS2 scans (Top Speed) to isolate and fragment the most abundant precursor ions by higher energy collisional dissociation (30% normalized collision energy, NCE). The resulting fragment ions were measured at a resolution of 10,000. Ions with +1 or unassigned charge were excluded from the analysis, and previously interrogated precursor ions were excluded using a dynamic window of 30s.

For the three unlabeled samples run on the Orbitrap Lumos mass spectrometer (Figure S5), peptides were loaded onto a PepMap 100 C18 pre-column (5 µm particle, 100 Å pore, 300 µm × 5 mm, Thermo Scientific) at 10 µL/min for 3 min with 0.1% formic acid. Peptides were separated on a reverse-phase nano EASY-spray C18 analytical column (2 µm particle, 100 Å pore, 75 µm × 500 mm, Thermo Scientific) with a gradient of 1.6% to 32% acetonitrile in 0.1% formic acid over 120 minutes at a flow rate of 300 nL/min. All *m/z* values of eluting ions (range

between 375-1500 Da) were measured at a resolution of 120,000. The MS1 scan was followed by data-dependent MS2 scans (3 second cycle time) to isolate and fragment the most abundant precursor ions at 35% NCE. Fragment ions were measured at a resolution of 15,000. Ions with +1 or unassigned charge were excluded from the analysis, and dynamic exclusion of previously interrogated precursor ions was 70s.

For the two SILAC samples run on the Orbitrap Q Exactive mass spectrometer, peptides were loaded onto a PepMap 100 C18 pre-column (5 µm particle, 100 Å pore, 300 µm × 5 mm, Thermo Scientific) at 10 µL/min for 3 min with 0.1% formic acid. Peptides were separated on a reverse-phase nano EASY-spray C18 analytical column (2 µm particle, 100 Å pore, 75 µm × 500 mm, Thermo Scientific) with a gradient of 1.6% to 32% acetonitrile in 0.1% formic acid over 120 minutes at a flow rate of 300 nL/min. All *m/z* values of eluting ions (range between 380-1500 Da) were measured at a resolution of 70,000. The MS1 scan was followed by data-dependent MS2 scans (Top 20) to isolate and fragment the most abundant precursor ions at 32.5% NCE. Fragment ions were measured at a resolution of 35,000. Ions with +1 or unassigned charge were excluded from the analysis, and dynamic exclusion was 60s.

Reproducibility of semi-quantitative protein abundance estimates

Initial samples were collected and analyzed using an Orbitrap Fusion Tribrid. To assess depth of coverage across collection points with varying amounts of sperm, three gel slices for the bursa and four or five gel slices for the seminal receptacle were analyzed following 1D SDS-PAGE gel fractionation. Protein abundances (NSAFs) between the 2-hour seminal receptacle replicates were significantly correlated (Pearson's $r = 0.95$), indicating high quantitative reproducibility. Due to the inherent difficulty in isolating sufficiently large sperm protein samples at the 4-day

collection points (1200 total dissections required), subsequent samples were analyzed using additional MS/MS runs (seven 1D SDS-PAGE gel slices) on a more sensitive Orbitrap Lumos. A principal component analysis (PCA) on protein abundances clearly highlights variation associated with increased sensitivity for samples analyzed on the Orbitrap Lumos, as captured by PC1 (46.2% of the variation explained; Fig. S5). PC2 captures consistent variation between samples purified from the bursa and sperm storage organs (28.8% variation explained). To maximize quantitative accuracy, comparisons between collection points were based on peptide spectral matches combined across replicates. Despite the fact that protein abundance estimates were derived from sperm purified from discrete spatiotemporal collection points (where substantial biological variation was expected), there was still high levels of quantitative reproducibility between samples, such as those isolated from different storage collection points (2-hour seminal receptacle vs 4-day seminal receptacle: $r = 0.94$, 4-day seminal receptacle vs 4-day spermatheca: $r = 0.94$).

Expansion of the *Drosophila melanogaster* sperm proteome

Given the increased sensitivity of mass spectrometry-based proteomic methodologies since the previous characterization of the *Drosophila melanogaster* sperm proteome (DmSP-II; 1), we conducted a new proteomic analysis of sperm to expand sperm proteome coverage. Flies (*D. melanogaster* w^{1118}) were maintained on standard cornmeal medium at ambient light and room temperature and collected within 24 hours of eclosion. Sperm samples were collected from 7-day old virgin and mated males. Virgin males were aged in vials for 7 days and then frozen in liquid nitrogen. Mated males were aged in vials for 3 days (to become sexually mature), paired with an excess of females for 2 days, separated from females and aged in fresh vials for an additional 2

days, and then frozen in liquid nitrogen. Sperm were isolated from seminal vesicles as described in Wasbrough et al. (1). Sperm from approximately 300 males were pooled in PBS per replicate, and two biological replicates were collected and analyzed per condition.

Sperm samples were resuspended in NuPAGE LDS sample buffer with NuPAGE reducing agent (Thermo Fisher) and solubilized by heating. Samples were separated by 1D SDS-PAGE, digested with trypsin, and analyzed by LC-MS/MS using an Orbitrap Q Exactive mass spectrometer as described above. RAW spectral data from virgin and mated samples were run together in a combined analysis using PEAKS X+, and the mass spectra were searched and filtered as described in the main text. This analysis identified 1412 high-confidence proteins which, when combined with DmSP-II, resulted in an updated and expanded canonical sperm proteome containing 2105 proteins (Dataset S1).

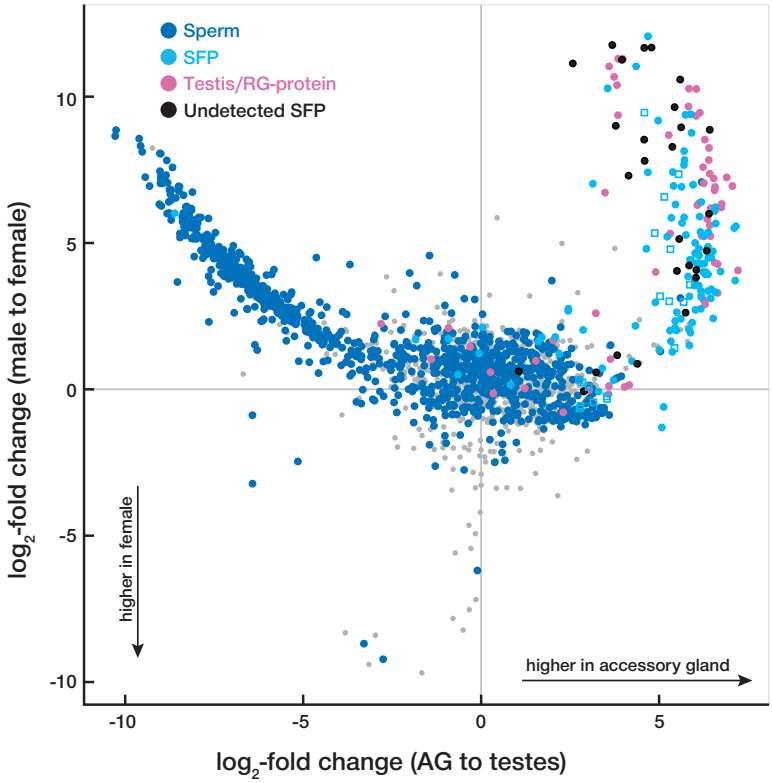

Figure S1. Numerous highly expressed SFPs do not associate with sperm. Tissue-biased expression versus sex-biased expression for all 1969 proteins identified in the bursa 30 minutes after mating. Sperm proteins are plotted in dark blue, Testis/RG-proteins in pink, SFPs in light blue, novel SFPs as blue squares, and undetected SFPs in black. Twenty-seven SFPs are plotted that are transferred to females (2) and highly expressed in the male accessory glands (log_2-fold change > 1) but are not detected in our study because they do not (or only weakly) associate with sperm.

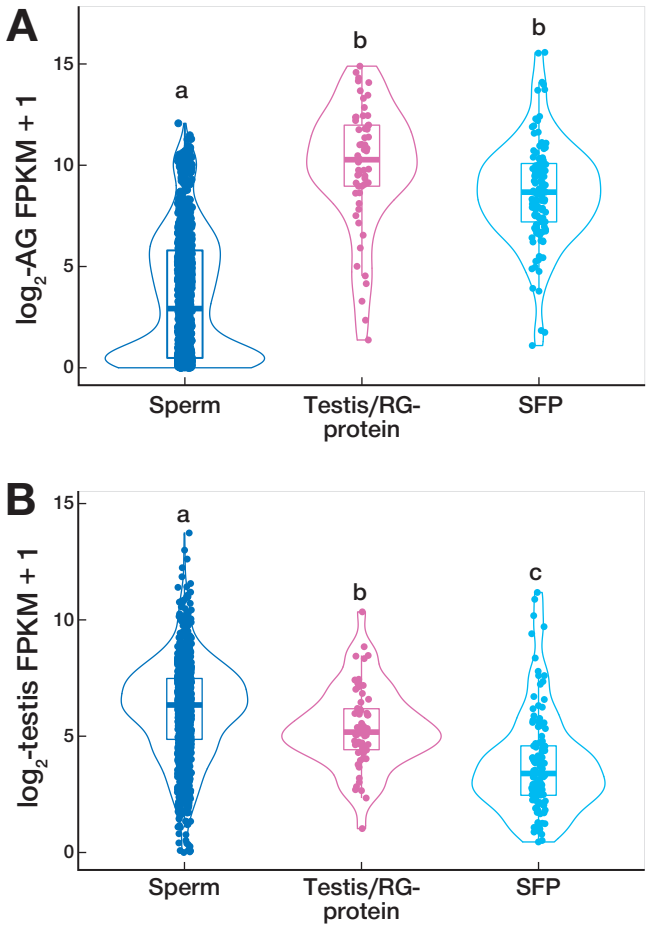

Figure S2. Sperm proteins and proteins derived from the male reproductive glands are not entirely discrete. Violin plots comparing the distributions among sperm, Testis/RG-proteins, and SFPs in **A**) absolute accessory gland (AG) expression and **B)** absolute testis expression. Letters above the violin plots denote distributions that are significantly different from each other (Kruskal-Wallis and post-hoc Dunn's tests, $p < 0.05$).

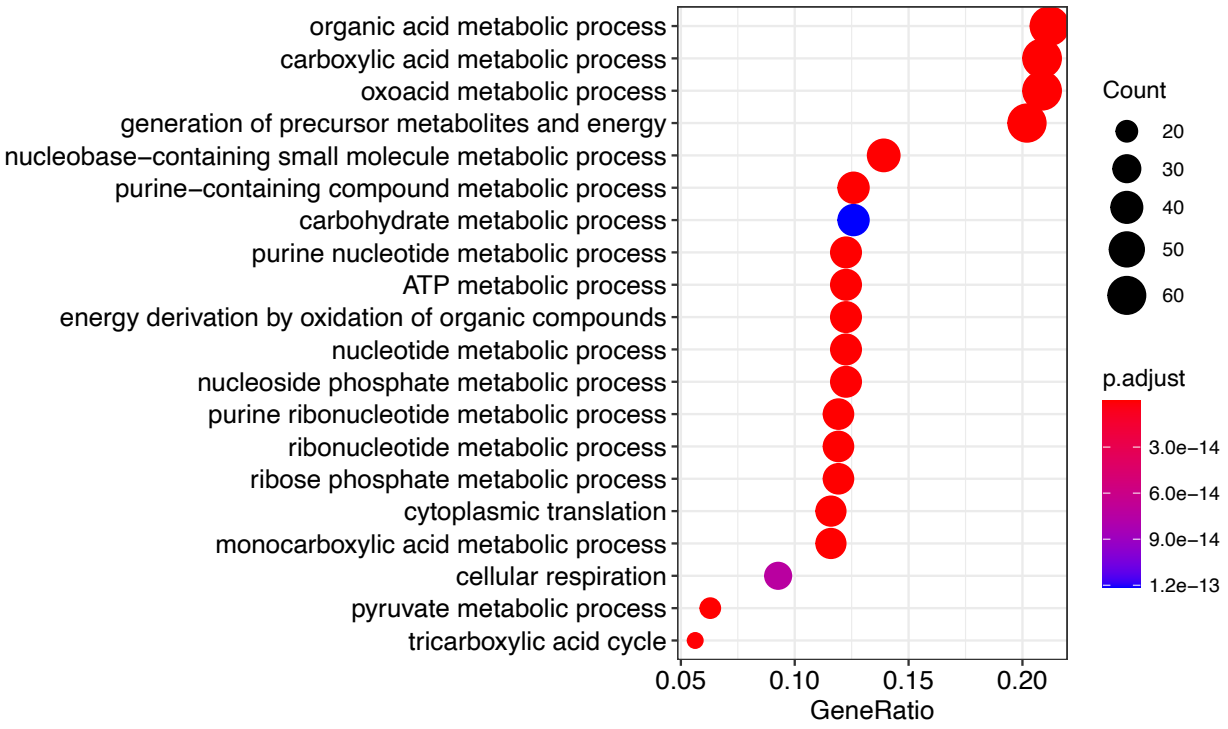

Figure S3. Female-derived sperm-associated proteins (i.e., both dual-derived sperm proteins and uniquely female proteins) are enriched for biological processes associated with energy metabolism. Dot plot depicting the 20 most enriched terms using clusterProfiler v4.0. Gene Ontology enrichment analysis was conducted using female-derived sperm-associated proteins as the input dataset and the FRT transcriptome as the background dataset. Dot color indicates the Benjamini-Hochberg adjusted p-value and dot size indicates the number of proteins associated with each term. GeneRatio is the proportion of input proteins associated with a given term.

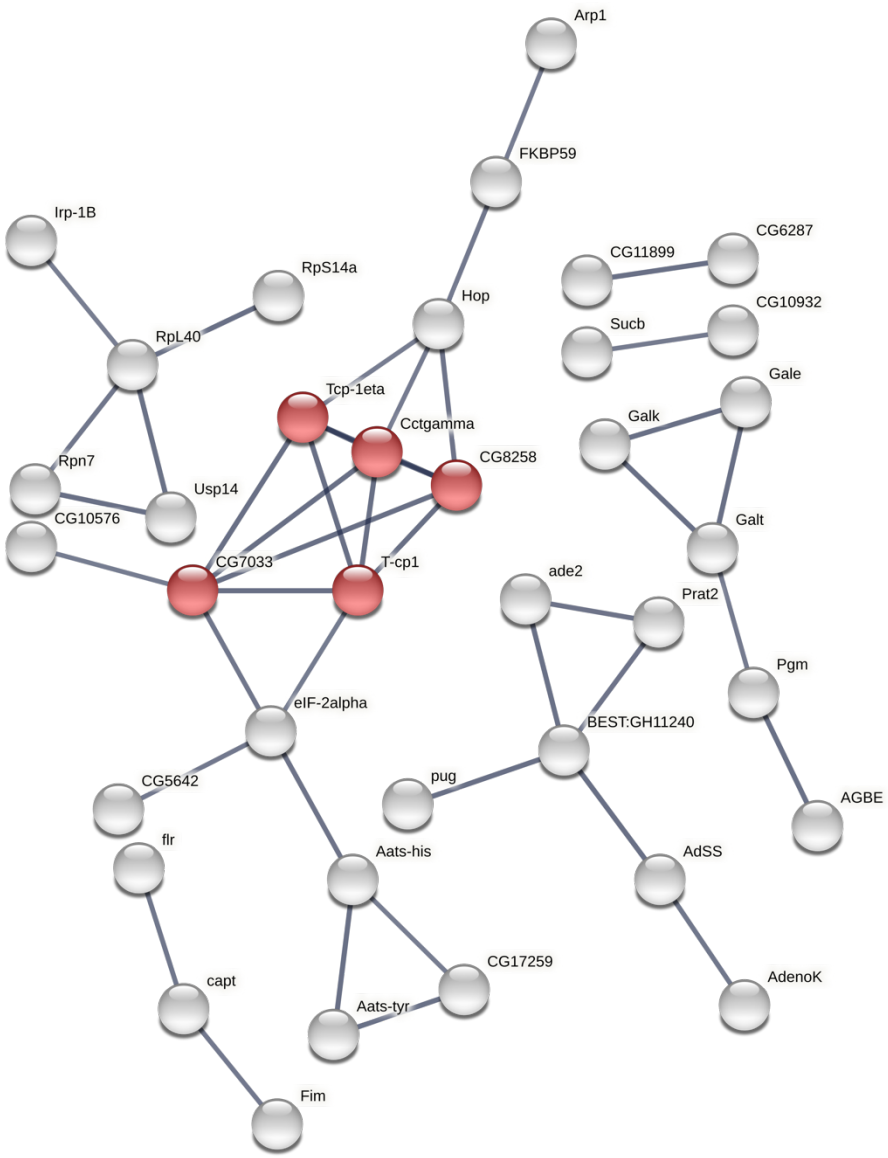

Figure S4. Uniquely female protein network. STRING analysis revealed a highly connected and significant protein interaction network among uniquely female sperm-associated proteins (3.9-fold enrichment in edges; PPI enrichment p-value: 7.74e-14). Notable is the hub of chaperonin-containing TCP1 complex proteins (highlighted in red) which have characterized functions in sperm surface remodeling in mammals (3).

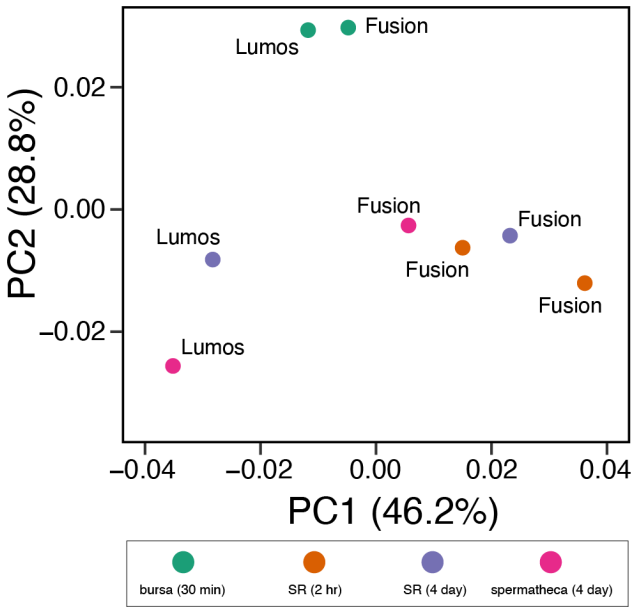

Figure S5. Principal component analysis biplot of protein abundances (NSAFs) for all 2339 proteins from the eight unlabeled sperm samples. Colors correspond to the four collection points: cyan = bursa at 30 minutes; orange = seminal receptacle at 2 hours; purple = seminal receptacle at 4 days; pink = spermatheca at 4 days. Points are labeled with the mass spectrometer on which each sample was analyzed (Orbitrap Lumos or Orbitrap Fusion). PC1 captures variation associated with the increased sensitivity for samples analyzed with the Lumos Orbitrap. PC2 separates samples between those purified from the bursa and sperm storage organs.

REFERENCES

1. Wasbrough, E. R., S. Dorus, S. Hester, J. Howard-Murkin, K. Lilley, E. Wilkin, A. Polpitiya, K. Petritis, and T. L. Karr. 2010. The *Drosophila melanogaster* sperm proteome-II (DmSP-II). J Proteom 73:2171–2185.
2. Wigby, S., N. C. Brown, S. E. Allen, S. Misra, J. L. Sitnik, I. Sepil, A. G. Clark, and M. F. Wolfner. 2020. The *Drosophila* seminal proteome and its role in postcopulatory sexual selection. Philos Trans R Soc Lond B 375:20200072.
3. Dun, M. D., N. D. Smith, M. A. Baker, M. Lin, R. J. Aitken, and B. Nixon. 2011. The chaperonin containing TCP1 complex (CCT/TRiC) is involved in mediating sperm-oocyte interaction. J Biol Chem 286:36875–36887.